applied sciences

MDPI

Type of the Paper (Article)

Multidisciplinary approach to evaluate the geochemical degradation of building stone related to pollution sources in the Historical Centre of Naples (Italy)

Valeria Comite [1✦], Michela Ricca [2✦], Silvestro Antonio Ruffolo [2], Sossio Fabio Graziano [3], Natalia Rovella[2], Concetta Rispoli [4], Chiara Gallo [5], Luciana Randazzo [2], Donatella Barca [2], Piergiulio Cappelletti [4] and Mauro Francesco La Russa [2*]

[1] University of Milan, Department of Chemistry, 20133 Milan (Italy); valeria.comite@gmail.com
[2] University of Calabria, Department of Biology, Ecology and Earth Sciences (DiBEST), 87036 Arcavacata di Rende, CS (Italy); michela.ricca@unical.it; silvestro.ruffolo@unical.it; donatella.barca@unical.it; natalia.rovella@unical.it; mlarussa@unical.it
[3] University of Naples, Federico II, Department of Pharmacy, 80138 Napoli (Italy); sossiofabio.graziano@unina.it
[4] University of Naples Federico II, Department of Earth Science, Environment and Resources (DiSTAR), 80138 Napoli (Italy); piergiulio.cappelletti@unina.it; concetta.rispoli@unina.it
[5] University of Salerno, Department of Chemistry and Biology, 84084 Fisciano, SA (Italy); chgallo@unisa.it

✦ These authors contributed equally to the work
* Correspondence: mlarussa@unical.it

Received: date; Accepted: date; Published: date

Abstract: Since ancient time the ability in construction is what identified and expressed the evolution of techniques, styles and raw materials used for historic buildings, highlighting great skills in stones processing. The use of geological materials in architecture is, therefore, a practice that has its roots as a bridge from past to today.
The present work is focused on the minero-petrographic and geochemical characterization of black crusts (BCs) samples taken from the historical centre of Naples, after selecting two pilot monumental areas. The latter have been chosen based on their historical importance, type of material, state of preservation and position in the urban context (i.e. high vehicular traffic area, limited traffic area, industrial area etc.). The construction building materials used and their interaction with environmental pollutions were studied comparing the results obtained by means of different analytical techniques such as polarized light Optical Microscopy (OM), scanning electron microscopy with energy dispersion system (SEM-EDS), X-ray powder diffraction (XRPD) and laser ablation coupled with inductively plasma mass spectrometry (LA-ICP-MS).

Keywords: black crusts; Cultural Heritage; marble, Naples pollution; heavy metals

1. Introduction

Air pollution strongly affects integrity of stone materials, since it promotes their degradation over time, especially in an urban context [1-9]. The formation of black crusts, which occurs mainly on carbonate rocks, represents one of the most dangerous degradation form caused by air pollution [10-18]. Generally their formations is due to calcium carbonate ($CaCO_3$) sulphation as a consequence of pH value decrease caused by SO_2 in the polluted atmosphere [19]. This dissolution let precipitate gypsum ($CaSO_4$ H_2O) that despite its water solubility remains as a crust that become black (due to soot particles) on surfaces protected from intense wash-out [20-23].

The formation of gypsum on the stone surface is a very rapid process and can be also accelerated by the deposition of particulate matter that being rich in metals and metal oxides, can act as a catalyst in the sulphation reaction.

Moreover, the difference in microstructure and porosity of the black crust related to the substrate leads to detachment of black crust itself, and as consequence weaks the stone, from the monuments' surface. [24-26]. Also, carbonaceous particles emitted by combustion processes (dark grey-black colour) are the main factors responsible for the blackening of buildings [27].

Recently, the study of black crusts has interestingly developed [12,26,28-32] Besides, research related to atmospheric deposit composition permits to understand the major causes of pollution, alongside an identification of the possible sources of pollutant emission in the area around a monument [33-34].

The characterization of black crusts on built heritage has a dual purpose. On one hand, there is a chance to understand the degree of decay of stone material in terms of microstructural features and chemical and mineralogical compositions. This can be useful for choosing a proper restoration procedure. On the other hand, these analyses can provide information about air pollution of the nearby environment, since the black crusts themselves can act as passive samplers of pollutants, with particular reference to metals [22-23,25-32].

In this paper, the analysis of black crusts coming from two monumental and historical sites located in the city of Naples is reported. As far as it is known, it is the first time that black crusts coming from this city have been analyzed. The city of Naples is located in southern Italy, Campania region, and is the third largest city of Italy following Rome and Milan, with high density population with the related consequences. High pollution rates due to intense and slowed motor vehicle traffic, characterize the urban downtown. According to the City Council, around 2 348 208 vehicles pass through the urban area every day (data ISTAT 2020). Moreover, there is a large port close to the centre, and several industrial areas roughly 10 km from the city centre. The historical city is the largest in Europe and has been designated as a UNESCO World Heritage Site [35].

Within the built Heritage of the urban centre, the sites selected for investigations are the complex of *San Domenico Maggiore* and some sculptures of the cloister of *San Marcellino e Festo* forming part of the homonym religious complex [36].

The choice of the two sites with different exposure in the Naples urban context was made to detect variability in the degradation forms, mainly due to the air pollution phenomena. On the fact, the complex of *San Domenico Maggiore* is a clear of historical monument example located in a high vehicular traffic area; on the contrary, the sculptures of the cloister of *San Marcellino and Festo*, although located outdoor, they are currently located in a restricted traffic area [36].

The church of San Domenico Maggiore is one of the most important religious complexes of Naples (Fig. 1a; 1b). It was built between the XIII and the XIV century by Charles II of Anjou, becoming the motherhouse of the Dominican friars of the Kingdom of Naples and church of the Aragonese nobility [37]. The church was erected according to the classic canons of the Gothic style, which was however compromised due to the numerous interventions that followed over the centuries, which altered its structure and the original Gothic forms, with three naves, side chapels, a large transept and a polygonal apse. The complex was restored several times; the last one started in 2000 and concluded in 2011 [37] The building is made mainly of Neapolitan yellow tuff, with some elements, such as the portal made of marble, the buttresses in *Piperno*, and part of the central space of the apse jutting out covered in red bricks [38].

The cloister of *San Marcellino e Festo* is part of a monastic complex dating back to the early Middle Ages (Fig. 1c; 1d) which along the centuries has undergone several renovations and restoration interventions (reference). An important restoration work was designed and carried out, in 1779, by Luigi Vanvitelli [36,39], especially affecting the consolidation of the dome and the majolica restoration, the extension of the southern portico of the cloister and the construction of an oratory. The cloister has a rectangular plan with arches supported by columns made of *Piperno*, with a central monumental garden enriched with fountains and marble sculptures [36].

The present work focuses on the minero-petrographic and geochemical characterization of several black crust samples collected from the above-mentioned sites and investigated using optical and electron microscopy, X-ray powder diffraction and laser ablation inductively coupled plasma-mass spectrometry.

The above reported integrated analytical approach allowed to obtain the main features of 1) black crusts and 2) underlying stone substrate, in terms of micromorphology, mineralogical composition and major and trace elements. Thanks to this wide-range characterization, valuable information on the formation processes of black crusts, as well as on interaction between stone substrate and the environment were studied. Specifically, valuable environmental data were obtained thanks to the identification of heavy metals, which, as known, may contribute to the recognition of the main pollution sources, responsible for the building materials deterioration over time.

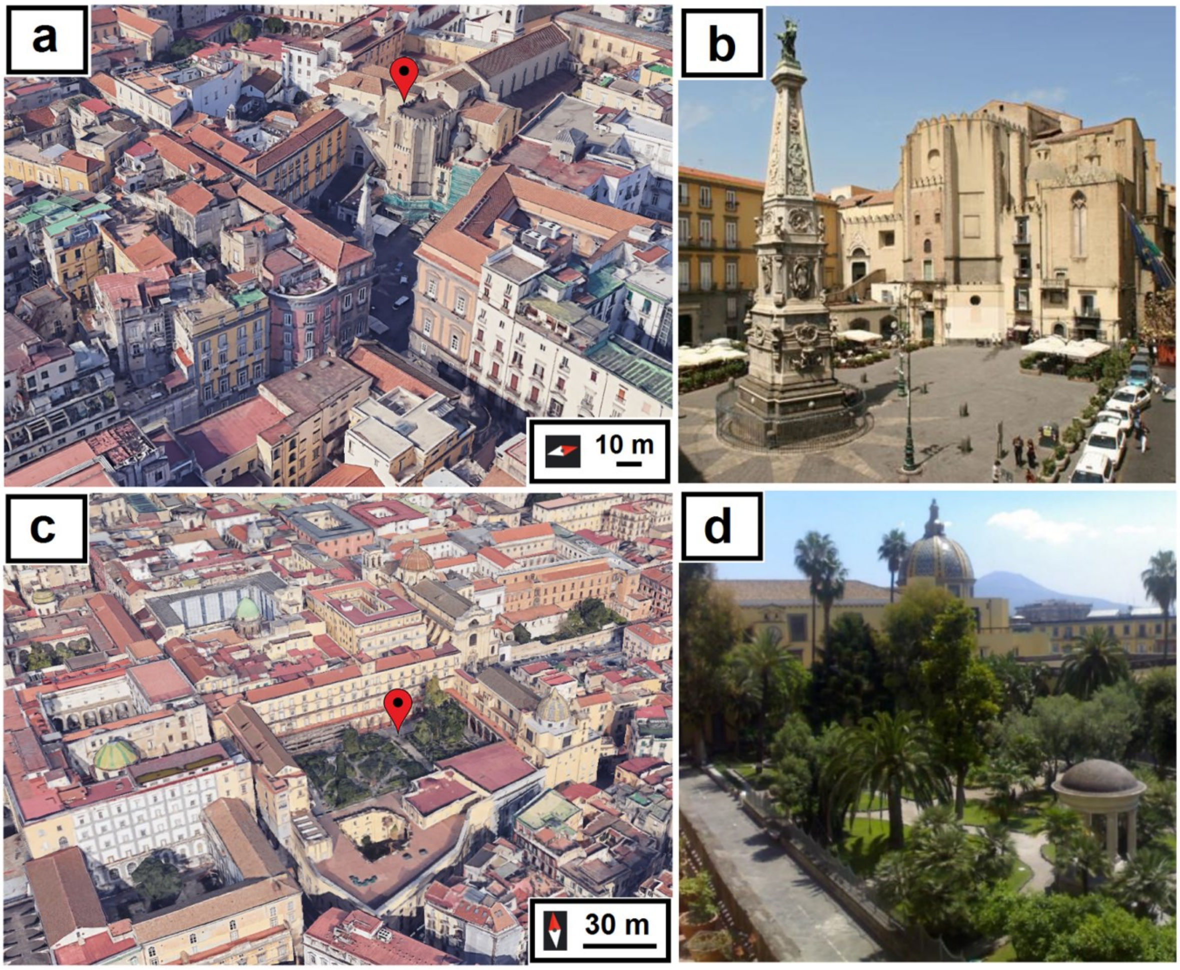

Figure 1. Complex of *San Domenico Maggiore* (40°50′55′′N; 14°15′16′′E) and cloister of *San Marcellino e Festo* (Naples, Italy) (40°50′49′′N; 14°15′28′′E): **a,c)** Aerial view of the two monumental complexes by Google Earth; **b)** view of the *San Domenico Maggiore* church with the façade facing the homonymous square; **d)** General view of the *Cloister* and *San Marcellino e Festo* church with evidence of tiled dome

2. Sampling

Eleven marble fragments were collected from different points at the two pilot sites, respectively four from the complex of *San Domenico Maggiore* and seven from the cloister of *San Marcellino e Festo*

(Fig. 2). Suitable stainless steel tools, such as lancets and small chisels, were used for sampling representative but non invasive portions of material affected by the presence of black crusts.

As concern the complex of *San Domenico Maggiore* (Fig. 2a; 2b; 2c), samples were retrieved from the façade of the church, specifically from marble portal located on the south-east side, alongside the apse of the church, overlooking *San Domenico* square.

From a first macroscopic observation, black crusts (SD series) looked rather homogeneous and compact, with a smooth surface and thin thickness. They also showed good adhesion to the underlying stone substrate, which was rather degraded, with evidence of swellings, poor compactness and sometimes powdery appearance.

Concerning the cloister of *San Marcellino e Festo* (Fig. 2d; 2e; 2f), samples were taken from the large and square plan monumental cloister, enriched with a garden adorned with marble fountains, statues, and various artefacts. The seven samples were taken from 3 different sculptures, respectively one sample from a marble well (SM-P series) (Fig. 2f), three from a marble structure with arches and pillars (SM-A series) (Fig. 2e), and three from a female marble bust (SM-S series) (Fig. 2d). Also in this case all black crusts showed a homogeneous and compact morphology, a very thin thickness and a good adhesion to the underlying stone substrate. As for the stone substrates, they looked fairly cohesive and slightly altered.

Samples with location description and heights is reported in Table 1

Table 1 List of the examined samples with a brief description.

Complex of *San Domenico Maggiore* (SD series)		
Sample ID	**Sampling location**	**Sampling heights**
SD1	Facade of the San Domenico church, main portal. Sampling on one of the left pillar (looking towards the portal), in a slightly curved area and on a vertical and external surface.	About 2.00 m from the planking level
SD2	Facade of the San Domenico church, main portal. Sampling on one of the right pillar (looking towards the portal), on a vertical and internal surface.	About 2.30 m from the planking level
SD3	Facade of the San Domenico church, main portal. Sampling on one of the right pillar (looking towards the portal), on an external corner.	About 1.60 m from the planking level
SD4	Facade of the San Domenico church, main portal. Sampling on one of the right pillar base (looking towards the portal), on a horizontal surface.	About 0.40 m from the planking level
Cloister of *San Marcellino e Festo* (SM-P, SM-A, SM-S series)		
Sample ID	**Sampling location**	**Sampling heights**
SM-P1	Monumental cloister, well. Sampling on a vertical surface, under the top edge.	About 1.00 m from the planking level
SM-A1	Monumental cloister, structure with arches and pillars. Sampling on a vertical surface, right column (looking towards the structure).	About 1.20 m from the planking level
SM-A2	Monumental cloister, structure with arches and pillars. Sampling on a convex surface, right side (looking towards the artefact), on a decorative element.	About 1.60 m from the planking level
SM-A3	Monumental cloister, structure with arches and pillars. Sampling on a vertical surface, on the base of the right column.	About 0.20 m from the planking level
SM-S1	Monumental cloister, female bust sculpture. Sampling on the veil, top of the head, on the back-side.	About 1.50 m from the planking level
SM-S2	Monumental cloister, female bust sculpture. Sampling on the veil, on the head, on the front-side.	About 1.50 m from the planking level
SM-S3	Monumental cloister, female bust sculpture. Sampling on a vertical portion of the bust, back-side.	About 1.50 m from the planking level

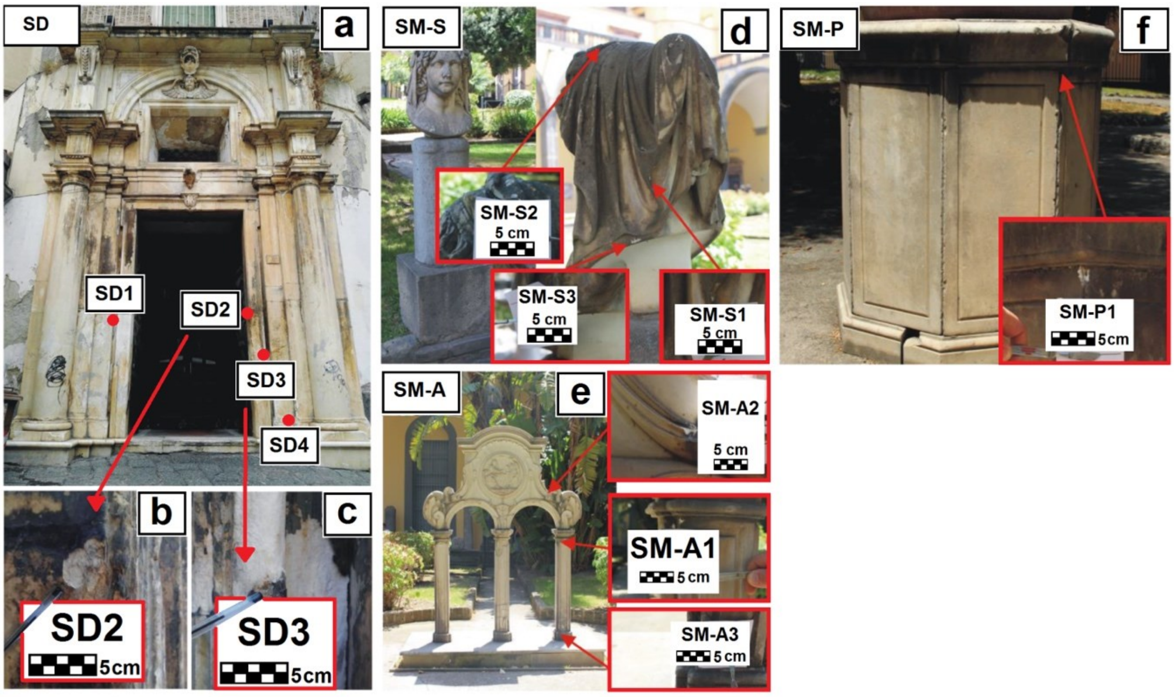

Figure 2. Sampling points of fragments collected at the: San Domenico Maggiore (**SD series**); Marble bust of the San Marcellino e Festo Cloister (**SM-S series**) Arch sculpture of the San Marcellino e Festo Cloister (**SM-A series**); Water well of San Marcellino e Festo Cloister (**SM-P series**).

3. Analytical methods

For a complete characterization of stone materials and degradation products (i.e. black crusts), several and complementary techniques were employed to investigate textural, morphological and compositional features as well as the interaction with rock substrate. Optical Microscopy (OM) observations were carried out on polished and stratigraphic thin sections by a Zeiss Axiolab microscope. OM allowed us to: **a)** determine the textural features; **b)** detect weathering grade on superficial layers by evaluating the morphology and growth of black crusts.

Scanning Electron Microscope (SEM) coupled with energy dispersive X-ray spectrometry (EDS) analyses were performed on polished cross-sections previously covered by carbon coating, to obtain information about micromorphology and chemical composition (in term of major elements) of the black crusts. Analyses were performed with a SEM 360 Cambridge Instruments Stereoscan, equipped with an EDAX microanalyser in energy dispersive spectrometry (EDS), with an ultrathin (UHT) window to ensure to detect light elements. The operating conditions were set at 20-kV accelerating voltages, 0.2-mA beam current, 100-s acquisition time, and 30–35 % dead time.

Chemical analyses were carried out according to standard mode and normalized in weight (%). The detection limits for the EDS system is approximately 0.1% weight. The accuracy of the analysis is periodically tested on standard USGS samples. Chemical analyses of the crust surfaces were performed in raster mode.

X-ray powder diffraction (XRPD), performed to investigate crusts mineralogical composition, were recorded on a D8 Advance Bruker X-ray diffractometer using X-ray Cu Kα radiation. Operative conditions were 40 kV voltage, 30 mA current, 0.02° 2θ step size, and 3.0 sec step time with a 2θ range of 10-80°.

Analyses of trace elements were performed by using laser ablation-inductively coupled plasma-mass spectrometry (LA-ICP-MS). This method allows detection and quantification of several elements with spot resolutions of approximately about 40–50 μm, leading to determination of compositional variations on a micrometric scale [40-42]. Measurements were performed by using an Elan DRCe instrument (Perkin Elmer/SCIEX), connected to a New Wave UP213 solid-state Nd-YAG laser probe (213 nm). The ablation was performed with spots of 40–50 μm with a constant laser repetition rate of 10 Hz and fluence of ~20 J/cm². Calibration was performed using the NIST 612-50 ppm glass reference material as the external standard [43]. Internal standardization to correct instrumental instability and drift was achieved using CaO concentrations from SEM-EDS analyses [44]. The accuracy was evaluated on BCR 2G glass reference material and on an in-house pressed-powder cylinder of the standard Argillaceous Limestone SRM1d of NIST [45]. The resulting element concentrations were compared with reference values from the literature [46]. The accuracy, as the relative difference from reference values, was always better than 12 %, and most elements plotted in the range of ±8 %. Analyses were performed on cross-sections 100 μm thick. Each sample was analyzed by several spot analyses depending on the thickness of the black crust, to assess the compositional variability within the crust and the differences between the degraded portion and the underlying unaltered substrate.

4. Results and discussion

4.1. Optical microscopy (OM) and mineralogical analysis (XRD) of the stone materials and the black crusts

OM allowed us the characterization, by microscopic point of view, of the collected samples: Complex of San Domenico Maggiore (SD series) and the cloister of *San Marcellino e Festo* (SM-P, SM-A, SM-S series). Observations, performed on most representative samples (i.e. SD2, SD3, SM-P1, SM-A1 and SM-S1) were reported in Table 2 and samples were classified according to their physical features along with mineralogical substrate composition.

Regarding the stone substrate, all samples can be classified as marbles with a fine grain size (Maximum Grain Size < 1 mm) (Fig. 3); fabric can be defined as "mosaic" type, with tiny to very tiny crystal size, often forming triple junctions at 120° [47]. The texture is homeoblastic (Ho) in SD2, SD3 (i.e. samples from the complex of *San Domenico Maggiore* – the portal) and SM-P1 (i.e. sample from the cloister of *San Marcellino e Festo* – the well) samples, while it is heteroblastic (He) in SM-A1 and SM-S1 (i.e. respectively samples from the cloister of *San Marcellino e Festo* – the structure with arches and pillars and the female bust). The grain size ranges from 0.1 mm to 0.45 mm in SD2 and SD3, from 0.1 mm to 70 mm in SM-S1, from 0.1 mm to 0.47 mm in SM-A1 and from 0.1 mm to 0.55 mm in SM-P1. All samples, other than crusts, show also remarkable micro-cracks just at the interface substrate-crusts this confirming the evident weathering acting on these manufacts that will for sure lead to a complete detachment of the weathered part.

As for the black crusts, samples SD2 and SD3 (i.e. samples from the complex of *San Domenico Maggiore* – the portal) show three different layers (Fig. 3 samples SD2, SD3). Starting from the more external: a) a first layer of black crust, which has a homogeneous morphology, thickness ranging from around 350 and 10 μm, and a colour (PPL, plane polarized light) that varies from light brown to dark brown. Embedded, iron oxides and hydroxides were observed, together with black combustion particles (i.e. particles formed during combustion processes, containing sulphur compound and catalysts; once wetted, such particles will nucleate gypsum crystals and will remain embedded in a gypsum crust) of spherical, sub-spherical and prismatic shape (ranging in size from 80 to 10 μm); b) a layer of *scialbo* which shows a relatively homogeneous morphology with a thickness ranging from a maximum of about 3 mm to a minimum of about 800 μm, dark brown in colour and with a secondary porosity of about 20%. Besides, individual and small calcite crystals along with oxides have been identified inside the same layer; c) another layer of crust (Fig. 3) well adherent to the stone substrate and showing a compact morphology, and thin thickness that varies from about 400 to 60 μm and a light grey colour. The latter layer displays microcrystalline gypsum crystals, iron oxides and hydroxides, along with spherical, sub-spherical and prismatic black combustion particles (ranging in size from 80 to 10 μm) inside.

Regarding the samples collected from the cloister of *San Marcellino e Festo*, the SM-S1 and SM-A1 crusts have irregular morphology and jagged on the outer edge, mammelonar in some portions, with thickness ranging from 520 to 75 μm. The colour varies from dark grey to brown, due to the presence of iron oxides and hydroxides respectively. Also, spherical, sub-spherical and prismatic combustion particles (ranging in size from 85 to 10 μm) distributed evenly along the entire investigated surface are visible (Fig. 3 sample SM-S1).

Instead, SM-P1 crust (Fig. 3) sample shows a heterogeneous morphology, mostly compact, with a thickness ranging from 800 and 50 μm. Inside, iron oxides, hydroxides and well-distributed combustion particles (sizes between 125 and 25 μm) were recognized, providing an overall dark grey colour.

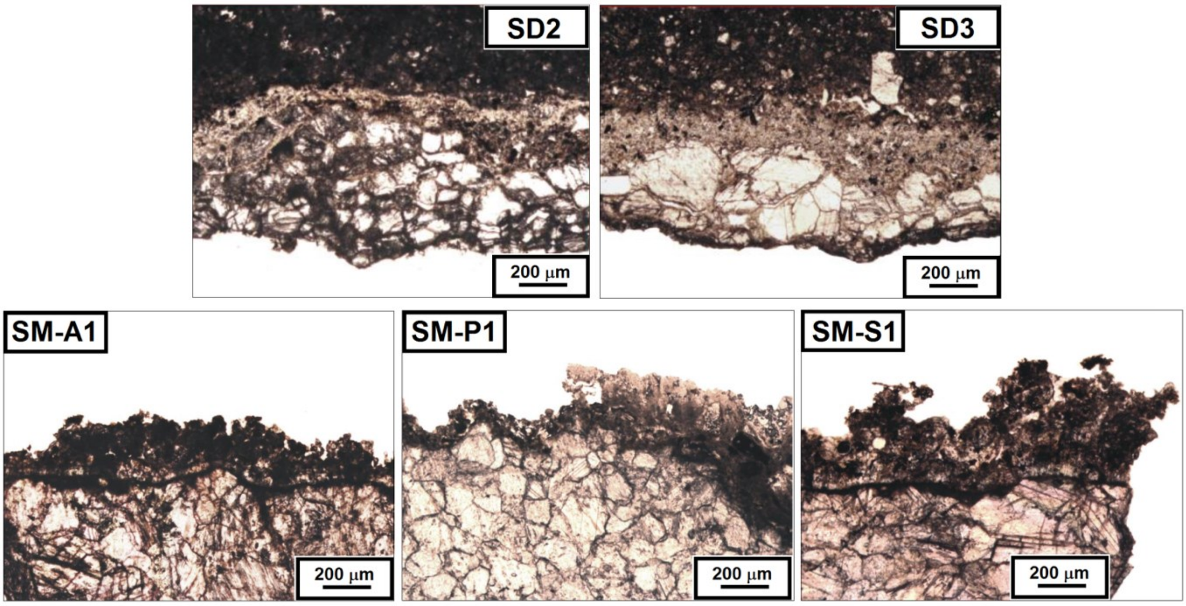

Figure 3. Microphotograph (OM, PPL) showing textural features of some selected marble fragments, with evidence of the black crust layer on the surface. SD2, SD3 are samples from the complex of *San Domenico Maggiore* while SM-A1, SM-P1 and SM-S1 were taken from the cloister of *San Marcellino e Festo*.

As regards mineralogical composition, results were reported also in Table 2. XRPD analyses were performed separately on substrate and on crusts evidencing that calcite is the main mineralogical phase for substrate (marble) and gypsum, along with whewellite and calcite traces, were present in all samples. Some differences were highlighted for samples SD3 and SM-A1 (presence of quartz and weddellite) along with SM-SA and SM-P1 (presence of weddellite).

According to the literature [48], the presence of calcium oxalates in the mineralogical forms of whewellite and weddellite, may depend on the restoration work carried out on the artefacts in past times.

Table 2 Main textural features of the examined samples (OM) along with the main mineralogical phase and accessory minerals (XRPD) occurring in the analysed samples and considering both unaltered substrate and black crusts.

Notes: Ca. calcite; Qtz. quartz; Gy. Gypsum; Whw. Whewellite; Wed. Weddellite; ++++. very abundant; +++. abundant; ++. moderate; +. poor; -. not present. Minerals abbreviations were made according to [49].

Complex of *San Domenico Maggiore* (SD series)									
Sample ID	**Grain Size μm**	**Texture**	**Fabric**	**Mineralogical phases in the substrate**	**Mineralogical phases in the black crust**				
					Ca	**Gy**	**Qtz**	**Whw**	**Wed**
SD2	450-100	Ho	Mosaic	Ca	+++	++	-	+	-
SD3	450-100	Ho	Mosaic	Ca	+++	++	+	++	-

Cloister of *San Marcellino e Festo* (SM-P, SM-A, SM-S series)									
Sample ID	**Grain Size μm**	**Texture**	**Fabric**	**Mineralogical phases in the substrate**	**Mineralogical phases in the black crust**				
					Ca	**Gy**	**Qtz**	**Whw**	**Wed**
SM-P1	550-100	Ho	Mosaic	Ca	++++	+++	-	++	+
SM-S1	690-100	He	Mosaic	Ca	++++	+++	-	++	+
SM-A1	470-100	He	Mosaic	Ca	++++	++	+	+	+

4.2. Micromorphological and elemental analysis of the black crusts by SEM-EDS

Scanning Electron Microscopy observations show many similarities between SD samples. Both show a stone substrate (US unaltered) overlayed by well adherent and homogeneous crusts with different thickness (Fig 4a; 4b). SD2 crust has a size that varies from 175 to 10 μm (Fig. 4a), while SD3 ranging from 150 to 5 μm (Fig. 4b).

Black crusts consist of gypsum, having acicular and lamellar crystal habit, where combustion particles of various sizes and morphology were identified (Fig 4c; 4d). Particles have a diameter ranging from 80 to 3 μm and they are spherical, sub-spherical, and irregular in shape and display smooth, porous or rough surface (Fig 4c). These are homogeneously distributed over the whole examined surface.

Micromorphological investigations on SM-S1 (Fig. 4e) showed a crust with variable thickness (from 520 to 75 μm), irregular and heterogeneous morphology. Inside, acicular-lamellar gypsum crystals and numerous combustion particles were recognized, the latter characterized by a morphology ranging from sub-spherical microporous to smooth spherical. Crust appears well adherent to the underlying substrate that is degraded and characterized by many micro-fractures.

SM-A1 (Fig. 4f) sample showed a crust well adherent to the substrate, with higher than others thickness (up to 350 μm), jagged outer edge and heterogeneous morphology. Acicular and lamellar gypsum crystals and few combustion particles were also recognized. The latter, ranging in size from 70 to 5 μm, have both partly sub-spherical morphology and porous surface and partly irregular morphology and rough surface.

Finally, SM-P1 sample (Fig. 4g; 4h) displays a poorly degraded stone substrate with a well adherent crust just in some points of the analyzed surface. The crust shows a heterogeneous and irregular morphology, with a thickness ranging from 790 to 50 μm (Fig. g), where lamellar gypsum and calcite crystals have been identified, probably coming from the stone substrate. Also, combustion particles having different shapes (spherical, sub-spherical and irregular), sizes (thickness between 2.5 and 125 μm) and surface morphologies (smooth, porous and wrinkled), distributed differently along the entire analyzed surface have been recognized (Fig. 4h).

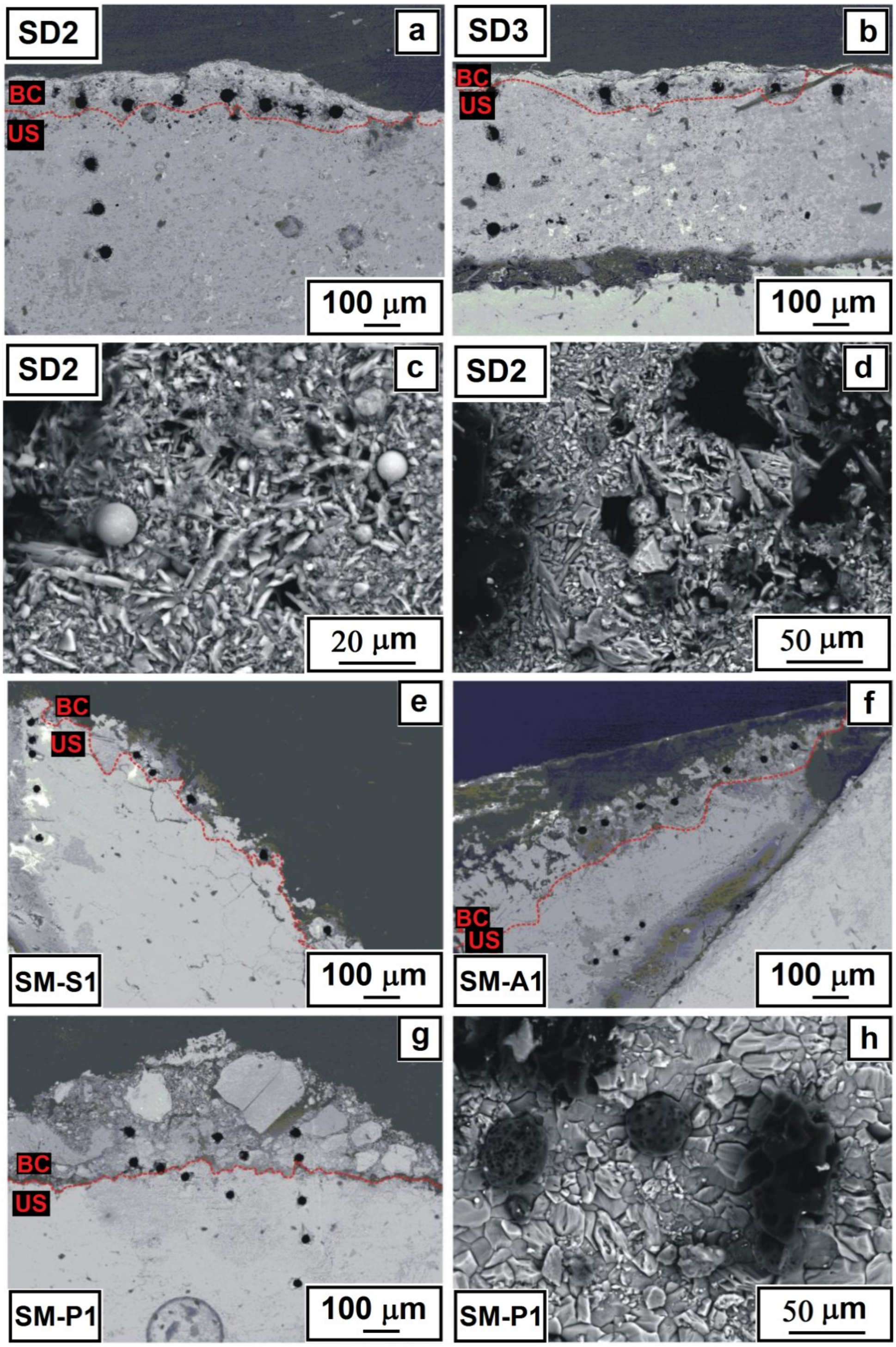

Figure 4. SEM microphotographs of some examined samples (i.e. SD2, SD3, SM-S1, SM-A1 and SM-P1) with details of combustion particles and gypsum crystals (Fig. 4c, 4d and 4h). The holes caused by LA-ICP-MS spot analyses (carried out on black crusts=BC and unaltered substrates=US) are also visible (Fig. 4a, 4b, 4e, 4f and 4g). The red dotted line demarcates the layer of black crust from the substrate.

To evaluate the chemical composition in terms of major elements, as well as their distribution within the sample, elemental analyses were carried out by EDS, on the surface of the black crust (BC).

Black crusts are mainly composed by SO_3 and CaO, clearly attributable to the gypsum. Also, SiO_2, Al_2O_3 and Fe_2O_3, along with smaller amounts of K_2O, P_2O_5, Na_2O, MgO and TiO_2, whose presence is ascribable to the abovementioned particles embedded into the crust (Table 3).

Since the SD2 and SD3 samples show crusts with similar composition, as well as SM-S1, SM-P1 and SM-A, in Table 3 is reported only the crust composition of the SD2 and SM-P1 samples, as representatives.

Table 3 Average concentrations of major elements (wt%) in the black crust of sample SD2 as representative of the complex of *San Domenico Maggiore* and SM-P1 as representative of the cloister of *San Marcellino e Festo.* Measurements were obtained by SEM-EDS analysis performed in raster mode.

	Complex of *San Domenico Maggiore*	**Cloister of *San Marcellino e Festo***
Major elements	**Sample SD2** **Average analysis No. 8**	**Sample SM-P1** **Average analysis No. 8**
Na_2O	<0.1	1.99
MgO	<0.1	1.19
Al_2O_3	6.70	8.82
SiO_2	7.82	13.60
P_2O_5	0.99	<0.1
SO_3	**40.90**	**38.60**
K_2O	3.49	2.50
CaO	**35.50**	**28.40**
TiO_2	<0.1	0.57
Fe_2O_3	5.59	4.36

To check distribution of SO_3 and CaO, detected in the analyzed window for SD2 and SM-P1, false colour maps were also obtained (Fig. 5a; 5b; 5c) as well as their combination (Fig. 5d).

Figure 5d further confirm that BC surface analyzed is mainly composed of gypsum, given by sulfur and calcium, with more marked yellow colouring, given by the combination of red and green colours (i.e. overlapping of red colours indicating 100% of S and green indicating 100% of Ca, according to their greater or lesser amount). Otherwise, the US surface shows a high concentration of calcium oxide, given by the greener colouring.

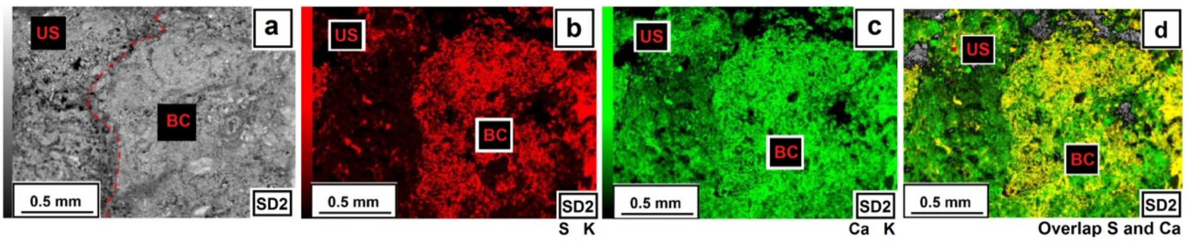

Figure 5. False-colour maps by SEM-EDS related to SD2 sample as representative. 5a. EDS analyzed window of the SD2 sample, consisting of the crust (BC) and stone substrate (US); 5b. distribution of S (red); 5c. distribution of Ca (green); 5d. overlapping and distribution map of S and Ca

4.3. Trace elements analysis by LA-ICP-MS

Chemical characterization of samples in terms of trace elements was performed using LA-ICP-MS technique on cross-sections with a polished surface.

The method allowed us to determine the trace elements both in the black crusts and the unaltered substrate (i.e. marbles) and a statistically valid number of analyses was always choose in function of sample thickness. Only for the SM-P1 sample, analyses were carried out only on the crust, due to the lack of representativeness of the substrate.

The average concentration (in ppm) of the most representative chemical elements, both in the unaltered substrate and in the black crusts, is reported in Table 4.

Major heavy metals concentrations detected in black crusts are related to chemical elements such as Ba, Cu, Pb, Ti and Zn; followed by other elements in smaller amounts.

Specifically, the BCs (SD2 and SD3) taken from the complex of *San Domenico Maggiore* show higher average maximum values in Pb (3525 ppm), Zn (1580 ppm) and Cu (224 ppm) than the substrate. In the same samples of BCs, similar and sometimes lower values of Ba, As and V, with respect to the unaltered substrate, were detected (Table 4).

As for the BCs, sampled from the cloister of *San Marcellino e Festo*, respectively SM-S1, SM-A1 and SM-P1, display lower concentrations in heavy metals compared to the previous ones (i.e. SD2 and SD3). In details, BCs of SM-S1, SM-A1 and SM-P1 show higher average maximum values in Ba (288 ppm), Ti (417 ppm), Zn (321 ppm) and Cu (93.5 ppm) than the unaltered substrate (Table 4).

The chemical concentration determined on the samples from the complex of *San Domenico Maggiore* show different concentrations according to sampling heights points. In particular, the SD2 sample taken at 2.30 m high, has a greater concentrations than SD3 sampled at 1.60 m high (Fig. 2), because it is located in an area protected from the wash-out (i.e. on a vertical and internal surface), thus favoring a greater accumulation of pollutants over time.

On the contrary, the black crusts belonging to the three historical artefacts from the cloister of *San Marcellino e Festo* (SM-S1, SM-A1 and SM-P1) exhibit different concentrations, attributable both to different sampling heights and to several exposure conditions and, consequently, to the different pollutants deposit.

Table 4. The average concentration (in ppm) of the most representative chemical elements, both in the unaltered substrate (US) and in the black crusts (BC)

	The Complex of *San Domenico Maggiore*						The Convent of *San Marcellino e Festo*											
	BC-SD2		BC-SD3		US-SD		BC-SMS1		US-SMS1		BC-SMA1		US-SMA1		BC-SMP1		US-SMP1	
Element	**Amount (ppm)**	**Std Dev**	**Amount (ppm)**	**Std Dev**	**Amount (ppm)**	**Std Dev**	**Amount (ppm)**	**Std Dev**	**Amount (ppm)**	**Std Dev**	**Amount (ppm)**	**Std Dev**	**Amount (ppm)**	**Std Dev**	**Amount (ppm)**	**Std Dev**	**Amount (ppm)**	**Std Dev**
As	48.46	2.10	36.52	2.17	51.63	12.23	5.59	0.60	1.72	0.51	7.89	1.36	2.33	-	9.09	1.46	2.70	0.73
Ba	938	91.18	1106	73.74	1104	232	139	32.44	6.93	1.68	288	26.09	9.15	0.30	190	67.82	16.27	7.71
Cd	1.19	0.07	0.86	0.07	0.54	0.10	0.59	0.07	0.77	0.16	0.58	0.17	0.44	-	1.44	0.15	0.63	0.22
Cr	22.75	1.14	17.80	0.69	26.94	6.24	12.00	1.97	5.22	0.71	20.89	0.91	15.31	-	8.71	1.17	2.89	0.61
Cu	224	24.61	60.08	4.02	18.18	3.69	93.54	21.10	4.44	2.69	26.17	6.23	1.23	0.28	45.06	8.40	52.32	5.97
Ni	10.31	0.61	8.02	0.77	7.68	1.45	11.54	2.73	1.06	0.29	3.56	0.65	0.68	0.20	6.06	1.18	10.44	0.90
Pb	3525	262	3134	292	82.09	23.49	85.55	7.87	17.37	8.04	109	6.67	37.02	5.20	122	11.69	147	6.36
Sb	25.59	1.75	12.71	1.21	6.73	1.15	5.84	1.07	0.19	0.01	1.65	0.41	0.11	0.04	2.01	0.94	0.48	0.24
Ti	1377	75.12	1023	63.80	1842	281	417	62.09	12.38	2.96	110	35.41	20.96	12.52	492	134	53.15	26.08
V	37.29	2.13	31.75	4.16	37.11	4.95	16.67	1.68	0.96	0.16	10.65	0.96	0.78	0.27	18.23	3.81	5.66	3.18
Zn	1580	197	589	52.97	32.00	2.07	321	26.73	19.25	7.05	169	53.64	26.62	1.74	481	62.21	904	24.13

To better understand how to discriminate between 1) elements ascribable to the deposition process from those 2) coming from the substrate, the enrichment factors (EFs) of chemical elements detected in black crusts compared with that revealed in the substrates, were calculated as the ratios of crust/substrate metals' concentration. Results are reported in Table 5.

Table 5 Enrichment factors (EFs) of the chemical elements detected in the black crusts

	Complex of *San Domenico Maggiore*		Cloister of *San Marcellino e Festo*		
Chemical elements	**Sample SD2**	**Sample SD3**	**Sample SM-S1**	**Sample SM-A1**	**Sample SM-P1**
As	0.9	0.7	3.3	4.6	5.2
Ba	0.8	1	20.1	41.6	38.4
Cd	2.2	1.6	0.8	0.8	5.5
Co	2	0.9	12.4	3.9	11.4
Cr	0.8	0.7	2.3	4	1.2
Cu	12.3	3.3	21.1	5.9	9.5
Ni	1.3	1	10.8	3.4	6.4
Pb	42.9	38.2	4.9	6.3	5.6
Sb	3.8	1.9	30.7	8.7	10.6
Ti	0.7	0.6	33.6	8.9	22.5
V	1	0.9	17.4	11.1	9.6
Zn	49.4	18.4	16.6	8.8	16.8

Generally, an enrichment factor lower or equal to 1 suggests that the source of the element coming from the substrate, while an enrichment factor greater than 1 may be imputable to an external "provenance", which means that elements are linked to a deposition process. Such a hypothesis is stronger as the enrichment factor increases.

Looking at Table 5 it is possible to observe these differences and in detail, cells in green show EFs values greater than 1, while red ones refer to values lower than 1.

High amount of Ba in the samples from the cloister of *San Marcellino e Festo* (SM-P, SM-A, SM-S series) probably may depend on restoration interventions [50] carried out in the past. About that, the barium hydroxide it was widely used for the conservative treatment of marbles in the past [51].

This thesis is supported by the investigations carried out by using OM. Thin section observations allowed to highlight the presence of a further layer between the marble substrate and the black crust (i.e. Fig. 3, sample SD3), almost certainly attributable to a restoration intervention; probably the same in which the barium was applied to consolidate the stone surface. This hypothesis is further supported by EF values (Table 5).

In particular, different EFs can be attributable to various factors such as the type of stone material, the particle deposit morphology (vertical surfaces), the different exposure to emission sources (mobile or fixed) and the wash-out phenomena. In this way, specimens SD2 and SD3 show a high enrichment factor in some elements such as Pb, Zn and Cu because they were sampled from the church portal which in the past was affected by mobile polluting sources and precisely vehicles.

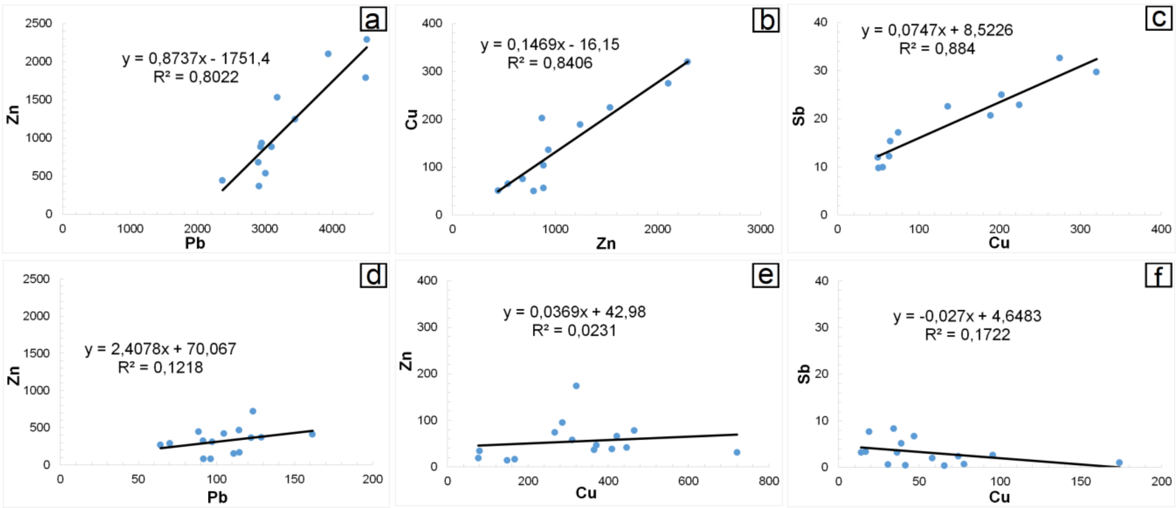

Figure 6. Correlation between the Zn vs Pb, Cu vs Zn e Sb vs Cu of the two different sites: a) b) c) Complex of *San Domenico Maggiore*; d) e) f) Cloister of *San Marcellino e Festo*

Figure 6 related to complex of *San Domenico Maggiore* (Fig. 6a; 6b; 6c) shows good correlations between the different heavy metals such as Zn vs Pb, Cu vs Zn and Sb vs Cu. In detail, the high correlation between Zn vs Pb (R2= 0.8022) agrees with the use of leaded gasoline as fuel for automotion [4] used up to a few decades ago. Moreover, the correlation between Cu vs Zn (R2= 0.8406) suggests an enrichment of the samples with tire wear particles and other parts of friction and machine wear [52-55]. Also, the latter could further indicate soil contamination from lubricating oil and exhaust emissions from vehicles [56-57]. Besides, the good correlation between Sb vs Cu (R2= 0.884) indicates a contribution from the brake wear [58-59].

On the contrary, the samples from the cloister of *San Marcellino e Festo* (SM-S1, SM-A1 and SM-P1) show a low correlation between the different heavy metals (Fig. 6d; 6e; 6f) suggesting differences in source.

As, Cr, Cu, Ni, Pb, Sb, Ti, V and Zn registered a moderate enrichment in all black crust samples (3 < EF < 33.6), which could be associated to different anthropogenic sources such as industrial activities [60-62], pavement wear [63] e vehicular traffic.

Some researches carried out on the atmospheric particulate matter and dusts sampled from the soil in Naples area [64-65] highlighted the presence of two different sources: mobiles and fixes. In particular, the last one can be related to the ILVA steel mill (working until 1993) located in the industrial area of Bagnoli-Coroglio and to the oil refineries (i.e. Q8, Esso, Tamoil) in the Eastern area of Naples. These industrial emissions have certainly affected the enrichment in some elements such as Ti, Zn, Pb, Cu, Ni and V. Furthermore, presence of high Sb values in these samples could be attributed to several incinerator plants [66] located at 30 km N to the city [67-68].

Besides, by comparing the low contents in As, Ni and V determined in this study with previous research [22,25-26,29,31-32,69], it is possible to assert that these values may depend on a moderate use of domestic heating due to the more temperate climate of Naples compared to that of other Italian and European cities.

In fact, the above-mentioned elements may be generally associated with the different fuels used in heating, such as the coal (in the past) or the fuel oils [70-71].

By comparing the data obtained from the investigations carried out in the two pilot sites, it is possible to assert that the greatest enrichment in heavy metals of the black crusts from the *church of San Domenico Maggiore* (samples SD2 and SD3) is certainly due to the use of Pb-based gasoline as well as the tire and brake wear and other parts machine wear. This aspect is also evident in Fig. 7, showing the location of the two cases-study in the Naples city centre. Particularly, the church of *San Domenico Maggiore* is nowadays located in a pedestrian area, forbidden to traffic only in the last decades (*Piazza San Domenico Maggiore and Vico San Domenico Maggiore*), and that in the past was an area with high vehicular traffic.

As concern samples from the cloister of *San Marcellino e Festo* (SM-S1, SM-A1 and SM-P1), data show an enrichment in different heavy metals that can be traced to different polluting sources (industrial activities and vehicular traffic). Sampled artefacts are located inside of a closed cloister and not exposed to direct sources of emissions, but they show anyway weathering phenomena related to stone decay and air pollution.

The achieved results highlight that all monuments, even those not directly exposed to sources of direct emissions, can undergo decay processes. In this way, it would be necessary to implement territorial policies for the protection of the cultural heritage, and above all that of historical interest.

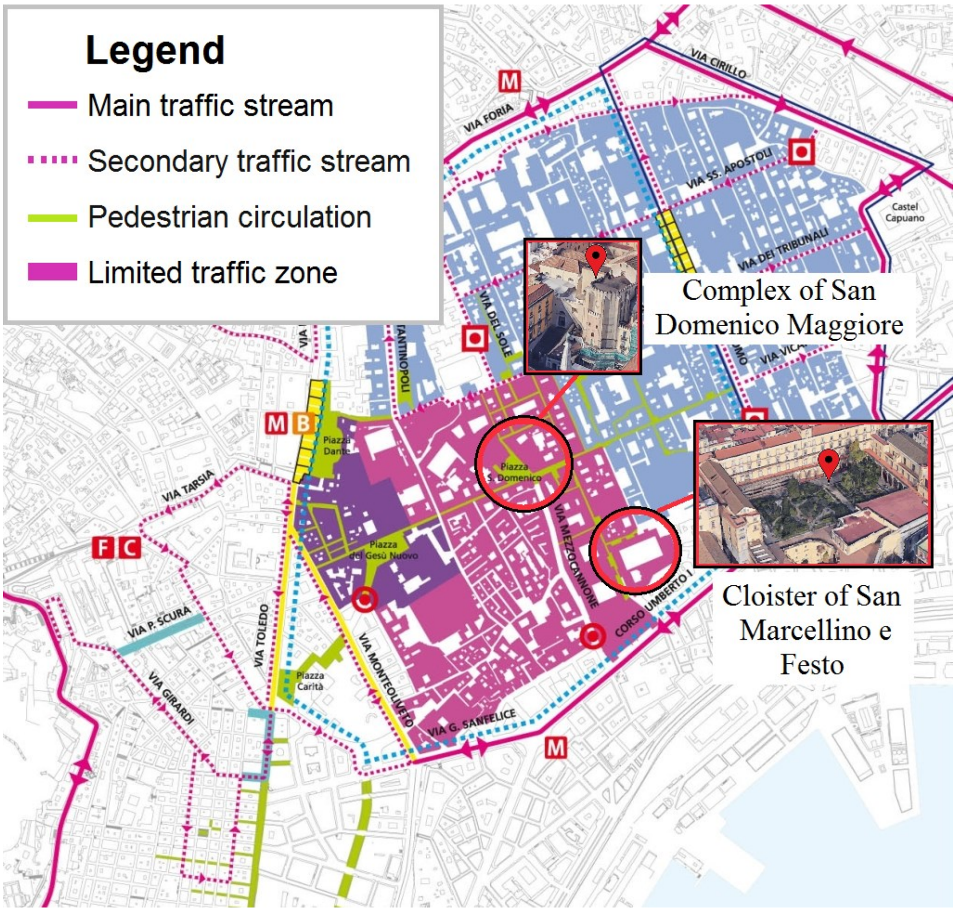

Figure 7. Road map of the urban city centre of Naples. The red circle indicates the location of the sampled monuments: SD = Complex of *San Domenico Maggiore*, SM = Cloister of *San Marcellino e Festo*.

5. Final remarks

In the present work, black crusts collected from two historical sites with different exposure within the city of Naples have been analysed in order to detect the variability in the degradation forms, mainly due to atmospheric pollutant.

Let's talk about the complex of *San Domenico Maggiore*, a historical monument located in a high vehicular traffic area and the ancient cloister of *San Marcellino e Festo*, located in a restricted traffic area. Sites were chosen to represent: on one hand a high vehicular traffic scenario and on the other a more protected (but always weathering affected) micro-environment.

The results achieved from the minero-petrographic and geochemical investigations made it possible:

- to highlight previous restorations and their effects of geomaterial overall conditions.
- to asses as the concentration of specific elements (such as As, Sb, Pb, Zn, Cu, Sn etc.) is sensibly higher in SD samples (from the complex of San Domenico Maggiore), testifying the fingerprint of air pollution due to vehicular emissions.
- to show as the As amount detected in the Naples city centre is lower than other Italian and European cities investigated in previous research, highlighting the importance of the impact of the local pollution sources on the cultural heritage.
- to draw considerations about conservations state of rock substrate. Some elements such as Zn, Cu, Ni, etc. are more present in substrate, testifying the presence of a net of microcracks that lead to move chemical elements from crusts to substrate. This mobility can lead also to the formation of new crusts contributing to accelerate the weathering damages.

The achieved results represent a further milestone to better manage future restoration intervention, especially in term of choice of the best cleaning procedures of historical and monumental complexes. Besides, suitable consolidation procedures will allow increasing the resistance of stone materials against the degradation phenomena mainly related to the geochemical mobility from the black crusts to substrate.

Author Contributions: Conceptualization, M.F.L.R.; P.C. and S.F.G; methodology, D.B.; M.F.L.R; formal analysis, M.R.; V.C; S.A.R; N.R. and L.R; investigation, M.R.; V.C; S.A.R; L.R.; C.R.; C.G.; data curation, M.R.; V.C; writing—original draft preparation, M.R. and V.C.; writing—review and editing, M.F.L.R.; P.C; S.F.G; supervision, M.F.L.R.; P.C. and S.F.G; funding acquisition, M.F.L.R.

All authors have read and agreed to the published version of the manuscript.

Conflicts of Interest: The authors declare no conflict of interest.

References

1. Amoroso, G.G.; Fassina V. Stone decay and conservation: atmospheric pollution, cleaning, consolidation and protection. Publisher: Elsevier: Amsterdam,1983**;** pp. 453.
2. Brimblecombe, P. *History of air pollution. In Urban Air Pollution – European Aspects*, Fenger, J., Hertel, O., and Palmgren, F., Eds., Publisher: Kluwer Academic Publishers Dordrecht, Boston, London; 1999, pp. 7-20.
3. Brimblecombe, P. Air pollution and architecture: Past, present and future. *J. Archit. Conserv.*, **2000,** *6(2),* 30-46. DOI:10.1080/13556207.2000.10785268.
4. Rodriguez-Navarro, C.; & Sebastian, E. Role of particulate matter from vehicle exhaust on porous building stones (limestone) sulfation. *Sci. Total Environ.*, **1996,** *187(2),* 79-91. DOI:10.1016/0048-9697(96)05124-8.

5. Antill, S. J.; & Viles, H.A. Aspects of Stone Weathering, Decay and Conservation, Proceedings of the 1997 Stone Weathering and Atmospheric Pollution Network Conference, **1999**, Jones, M.S. and Wakefield R.D., pp. 1-214.
6. Barone, G.; La Russa, M.F.; Lo Giudice, A.; Mazzoleni, P.; & Pezzino, A. The cathedral of S. Giorgio in Ragusa Ibla (Italy): Characterization of construction materials and their chromatic alteration. *Environ. Geol.*, **2008,** *55(3),* 499-504. DOI: 10.1007/s00254-007-0995-0.
7. Belfiore, C.M.; La Russa, M.F.; Pezzino, A.; Campani, E.; & Casoli, A. The baroque monuments of modica (eastern Sicily): Assessment of causes of chromatic alteration of stone building materials. *Appl. Phys. A,* **2010**, *100(3)*, 835-844. DOI:10.1007/s00339-010-5659-3.
8. Gulotta, D., Bertoldi, M., Bortolotto, S., Fermo, P., Piazzalunga, A., & Toniolo, L. The angera stone: A challenging conservation issue in the polluted environment of Milan (Italy). *Environ. Earth Sci.*, **2013,** *69(4),* 1085-1094. DOI:10.1007/s12665-012-2165-2.
9. Morra, V.; Calcaterra, D.; Cappelletti, P.; Colella.; A, Fedele, L.; de Gennaro, R.; Langella, A.; Mercurio, M.; de Gennaro, M. Urban geology: relationships between geological setting and architectural heritage of the Neapolitan area. *J Virtual Explor*, **2010,** *26,* 1- 36. https://doi.org/10.3809/jvirtex.2010.00261.
10. Del Monte, M.; Sabbioni, C.; & Vittori, O. Airborne carbon particles and marble deterioration. *Atmos. Environ.*, **1981,** *1967, 15(5),* 645-652. DOI:10.1016/0004-6981(81)90269-9.
11. Carta, L.; Calcaterra, D.; Cappelletti, P.; Langella, A.; de Gennaro, M. The stone materials in the historical architecture of the ancient center of Sassari: distribution and state of conservation. *J. Cult. Herit.*, **2005**, *6(3),* 277-286. DOI:10.1016/j.culher.2004.10.006.
12. Bonazza, A., Sabbioni, C., & Ghedini, N. Quantitative data on carbon fractions in interpretation of black crusts and soiling on European built heritage. *Atmos. Environ*., **2005**, *39(14),* 2607-2618. DOI:10.1016/j.atmosenv.2005.01.040.
13. Comite, V.; Barca, D.; Belfiore, C.M.; Bonazza, A.; Crisci, G.M.; La Russa, M.F.; Pezzino, A.; Sabbioni C. Potentialities of spectrometric analysis for the evaluation of pollution impact in deteriorating stone heritage materials, In *Rendiconti online della Società Geologica Italiana.* Critelli, S., Muto, F., Perri F., Petti, F.M., Sonnino, M., Zuccari, A. Eds., 86 Congresso Nazionale della Società Geologica Italiana, Arcavacata di Rende, 18–20 Settembre 2012, 21, pp 652–653.
14. Prikryl, R.; Svabodová, J.; Zák, K.; Hradil, D. Anthropogenic origin of salt crusts on sandstone sculptures of Prague's Charles Bridge (Czech Republic). Evidence of mineralogy and stable isotope geochemistry, *Eur. J. Mineral.* **2004**, *16*, 609–18. DOI: 10.1127/0935-1221/2004/0016-0609.
15. Torfs, K.; Van Grieken, R.E.; Buzek, F. Use of stable isotope measurements to evaluate the origin of sulfur in gypsum layers on limestone buildings, *Environ. Sci. Pollut. Res. 1997*, *31*, 2650–5. https://doi.org/10.1021/es970067v.
16. Vallet, J. M.; Gosselin, C.; Bromblet, P.; Rolland, P.; Vergés-Belmin, V.; Kloppmann W. Origin of salts in stone monuments degradation using sulphur and oxygen isotopes: first results of the Bourges Cathedral (France), *J. Geochem. Explor.* **2006**, *88,* 358–62. DOI 10.1016/j.gexplo.2005.08.075.
17. N. Schleicher, C. Recio, Source identification of sulphate forming salts on sandstones from monuments in Salamanca, Spain—a stable isotope approach, Environ. Sci. Pollut. Res. 17 (2010) 770–8. DOI 10.1007/s11356-009-0196-3.
18. Kloppmann, W.; Bromblet, P.; Vallet, J.M.; Vergès-Belmin, V.; Rolland, O.; Guerrot, C. Building materials as intrinsic sources of sulphate: a hidden face of salt weathering of historical monuments investigated through multi-isotope tracing (B, O, S), *Sci. Total. Environ.* **2011**, *409(9),* 1658–69. DOI 10.1016/j.scitotenv.2011.01.008.
19. de' Gennaro, M.; Colella, C.; Pansini, M. Hydrothermal conversion of trachytic glass into zeolite. II Reactions with high-salinity waters. *Neues Jahrbuch Far Mineralogie- Monatshefte*, **1993**, *3,* 97-110.
20. Maravelaki-Kalaitzaki, P., & Biscontin, G. Origin, characteristics and morphology of weathering crusts on Istria stone in Venice. Atmos. Environ., 1999, 33(11), 1699-1709. DOI:10.1016/S1352-2310(98)00263-5.
21. Kramar, S.; Mirtič, B.; Knöller, K.; Rogan-Šmuc, N.; Weathering of the black limestone of historical monuments (Ljubljana, Slovenia): oxygen and sulfur isotope composition of sulfate salts. *Appl Geochem,* **2011,** *26 (9–10),* 1632–1638. DOI: 10.1016/j.apgeochem.2011.04.020.
22. La Russa, M.F., Belfiore, C.M., Comite, V., Barca, D., Bonazza, A., Ruffolo, S. A., Pezzino, A. Geochemical study of black crusts as a diagnostic tool in cultural heritage. *Appl Phys A-Mater,* **2013,** *113(4),* 1151-1162. DOI:10.1007/s00339-013-7912-z.

23. Barca, D.; Comite, V.; Belfiore, C.M.; Bonazza, A.; La Russa, M.F.; Ruffolo, S.A.; Sabbioni, C. Impact of air pollution in deterioration of carbonate building materials in Italian urban environments. *Appl. Geochem.*, **2014,** *48,* 122-131. DOI: 10.1016/j.apgeochem.2014.07.002.
24. McAlister, J.J.; Smitha, B.J.; Tőrők, A. Transition metals and water-soluble ions in deposits on a building and their potential catalysis of stone decay. *Atmos Environ*, **2008**, *42*, 7657–7668.
25. Ruffolo, S.A., Comite, V., La Russa, M.F., Belfiore, C.M., Barca, D., Bonazza, A., Crisci, G.M., Pezzino, A., Sabbioni, C. Analysis of black crusts from the Seville Cathedral: A challenge to deepen understanding the relationship among microstructure, microchemical features and pollution sources, *Sci. Total Environ*. **2015,** *502,* 157–166.
26. La Russa, M.F., Fermo, P., Comite, V., Belfiore, C.M., Barca, D., Cerioni, A., De Santis, M., Barbagallo, L.F., Ricca, M., Ruffolo, S. A. The Oceanus statue of the Fontana di Trevi (Rome): The analysis of black crust as a tool to investigate the urban air pollution and its impact on the stone degradation. *Sci. Total Environ.*, **2017**, *593-594*, 297-309. DOI 10.1016/j.scitotenv.2017.03.185.
27. Fermo, P.; Gonzalez Turrion, R.; Rosa, M.; Omegna, A. A new approach to assess the chemical composition of powder deposits damaging the stone surfaces of historical monuments, *Environ. Sci. Pollut. Res.* **2015**, *22,* 6262–6270. DOI 10.1007/s11356-014-3855-y.
28. Belfiore, C.M., Barca, D., Bonazza, A., Comite, V., la Russa, M.F., Pezzino, A., Sabbioni, C. Application of spectrometric analysis to the identification of pollution sources causing cultural heritage damage. Environ *Sci Pollut Res*, **2013**, *20(12),* 8848-8859. DOI:10.1007/s11356-013-1810-y.
29. La Russa, M.F., Comite, V., Aly, N., Barca, D., Fermo, P., Rovella, N., Antonelli, F., Tesser, E., Aquino, M., Ruffolo, S.A. Black crusts on Venetian built heritage, investigation on the impact of pollution sources on their composition, *Eur. Phys. J. Plus,* **2018,** *133: 370,* DOI: 10.1140/epjp/i2018-12230-8.
30. Comite, V., Fermo, P. The effects of air pollution on cultural heritage: the case study of Santa Maria delle Grazie al Naviglio Grande (Milan). *Eur. Phys. J. Plus,* **2018,** *133(12),* 556. https://doi.org/10.1140/epjp/i2018-12365-6.
31. Comite, V., Pozo-Antonio, J.S., Cardell, C., Rivas, T., Randazzo, L., La Russa, M.F., Fermo, P. Metals distributions within black crusts sampled on the facade of an historical monument: The case study of the Cathedral of Monza (Milan, Italy). In 2019 IMEKO TC4 International Conference on Metrology for Archaeology and Cultural Heritage, MetroArchaeo, **2019**, 73-78
32. Comite, V., Pozo-Antonio, J.S., Cardell, C., Rivas, T., Randazzo, L., La Russa, M.F., Fermo, P. Environmental impact assessment on the Monza Mathedral (Italy): a multi-analytical approach. Int. *J. Conserv. Sci.*, **2020**, *11, Special Issue 1,* 291-304.
33. Ozga, I.; Ghedini, N.; Giosuè, C.; Sabbioni, C.; Tittarelli, F.; Bonazza, A. Assessment of air pollutant sources in the deposit on monuments by multivariate analysis. *Sci Total Environ.* **2014**, *490,* 776-784.
34. Smith, B.J., Török, A., McAlister, J.J., & Megarry, Y. Observations on the factors influencing stability of building stones following contour scaling: A case study of oolitic limestones from Budapest, Hungary. *Build Environ.*, **2003,** *38(9-10),* 1173-1183. DOI:10.1016/S0360-1323(03)00076-3.
35. AA. VV. Patrimoni e Siti UNESCO: Memoria, Misura e Armonia, Editor Gancemi; Italy; pp. 328-331
36. Di Benedetto, C.; Gautiero, A.; Guarino, V.; Allocca, V.; De Vita, P.; Morra, V.; Cappelletti, P.; Calcaterra, D. Knowledge-based model for geomaterials in the Ancient Centre of Naples (Italy): Towards an integrated approach to cultural heritage. Digital Applications in Archaeology and Cultural Heritage, in press https://doi.org/10.1016/j.daach.2020.e00146
37. Foglia, O.; Maietta I. La fabbrica di San Domenico Maggiore a Napoli. Storia e restauro. Editor Arte'm, Napoli, Italia; 2016.
38. Smylitopoulos, C. *Agents of Space: Eighteenth-Century Art, Architecture, and Visual Culture*. Editor Smylitopoulos, C., Eds Cambridge scholars publishing; 2016 pp 238
39. Fratta, A. Il Patrimonio architettonico dell'Ateneo Fridericiano (II volume). Editor Arte Tipografica, Napoli, Italia; 2004.
40. Gratuze, B. Obsidian characterization by laser ablation ICP-MS and its application to prehistoric trade in the Mediterranean and the near east: Sources and distribution of obsidian within the Aegean and Anatolia. *J. Archaeol. Sci.*, **1999,** *26(8),* 869-881. DOI:10.1006/jasc.1999.0459.
41. Vander Putten, E.; Dehairs, F.; André, L.; & Baeyens, W. Quantitative in situ microanalysis of minor and trace elements in biogenic calcite using infrared laser ablation - inductively coupled plasma mass

spectrometry: A critical evaluation. *Anal. Chim. Acta,* **1999,** *378(1-3),* 261-272. DOI:10.1016/S0003-2670(98)00613-8.

42. Wyndham, T.; McCulloch, M.; Fallon, S.; & Alibert, C. High-resolution coral records of rare earth elements in coastal seawater: Biogeochemical cycling and a new environmental proxy. *Geochim Cosmochim Ac.,* **2004,** *68(9),* 2067-2080. DOI: 10.1016/j.gca.2003.11.004.
43. Pearce, N.J.G.; Perkins, W.T.; Westgate, J.A.; Gorton, M.P.; Jackson, S.E.; Neal, C.R.; & Chenery, S.P. A compilation of new and published major and trace element data for NIST SRM 610 and NIST SRM 612 glass reference materials. *Geostandards Newslette,* **1997,** *21(1),* 115-144. DOI:10.1111/j.1751-908X.1997.tb00538.x.
44. Fryer, B.J.; Jackson, S.E.; & Longerich, H.P. The design, operation and role of the laser-ablation microprobe coupled with an inductively coupled plasma-mass spectrometer (LAM- ICP-MS) in the earth sciences. Canad Mineral, **1995,** *33(2),* 303-312.
45. Barca, D.; Belfiore, C.M.; Crisci, G.M.; La Russa, M.F.; Pezzino, A.; & Ruffolo, S.A. Application of laser ablation ICP-MS and traditional techniques to the study of black crusts on building stones: A new methodological approach. *Environ Sci Pollut Res*, **2010**, *17(8)*, 1433-1447. DOI: 10.1007/s11356-010-0329-8.
46. Gao, S.; Liu, X.M.; & Yuan, H.L. Determination of forty two major and trace elements in USGS and NIST SRM glasses by laser ablation-inductively coupled plasma-mass spectrometry. *Geostand. Newsl.,* **2002,** *26(2),* 181-196. https://doi.org/10.1111/j.1751-908X.2002.tb00886.x.
47. Lazzarini, L. Archaeometric aspects of white and coloured marbles used in antiquity: the state of the art *Per. Mineral.* **2004**, *73,* 113-125.
48. Cariati, F.; Rampazzi, L.; Toniolo, L.; Pozzi A. Calcium Oxalate Films on Stone Surfaces: Experimental Assessment of the Chemical Formation. *Stud Conserv*, **2000,** *45(3),* 180-188. DOI: 10.2307/1506764
49. Whitney, D.L.; Bernard, W. Evans. Abbreviations for names of rock-forming minerals. *Am Mineral,* **2010,** *95 (1),* 185–187 DOI: 10. 2138/am.2010.3371.
50. Fratta, A; AA.VV. *Il complesso di San Marcellino. storia e restauro*, Editor Fridericiana editrice universitaria, Napoli, Italia; 2000, pp 232.
51. Ashurst, J. *Conservation of Building and Decorative Stone,* Edotor Dimes, F.G.; Ashurst, J., Eds., Publisher: Elsevier LTD, Oxford, England, 1998; pp. 466.
52. Canepari, S.; Perrino, C.; Olivieri, F.; Astolfi, M.L. Characterisation of the traffic sources of PM through size-segregated sampling, sequential leaching and ICP analysis. *Atmos. Environ.,* **2008**, *42,* 8161-8175. https://doi.org/10.1016/j.atmosenv.2008.07.052.
53. Bukowiecki, N.; Lienemann P.; Hill, M.; Furger, M.; Richard, A.; Amato, F.; Prévôt, A.S.H.; Baltensperger U.; Buchmann, B.; Gehrig, R. PM10 emission factors for non-exhaust particles generated by road traffic in an urban street canyon and along a freeway in Switzerland. *Atmos. Environ.*, **2010,** *44(19),* 2330–2340. DOI: 10.1016/j.atmosenv.2010.03.039.
54. Brito, J.; Rizzo, L.V.; Herckes, P.; Vasconcellos, P.C.; Caumo, S.E.S.; Fornaro, A.; Ynoue, R.Y.; Artaxo, P.; Andrade, M.F. Physical-chemical characterisation of the particulate matter inside two road tunnels in the São Paulo metropolitan area. *Atmos Chem Phys,* **2013,** *13(24),* 12199– 12213. https://doi.org/10.5194/acp-13-12199-2013.
55. Dongarrà, G.; Manno, E.; Varrica, D.; Possible markers of traffic-related emissions, *Environ Monit Assess,* **2009,** *154,* 117–125. DOI: 10.1007/s10661-008-0382-7.
56. Aatmeeyata, Sharma, M., Polycyclic aromatic hydrocarbons, elemental and organic carbon emissions from tire–wear. *Sci. Total Environ.* **2010,** *408,* 4563–4568. https://doi.org/10.1016/j.scitotenv.2010.06.011
57. Cui, M.; Chen, Y.; Feng, Y.; Li, Ch.; Zheng, J.; Tian, Ch.; Yan, C.; Zheng, M. Measurement of PM and its chemical composition in real–world emissions from non–road and on– road diesel vehicles. *Atmos. Chem. Phys.*, **2017,** *17,* 6779–6795. https://doi.org/10.5194/acp-17-6779-2017.
58. Schauer, J.; Lough, G.; Shafer, M.; Christensen, W.; Arndt, M.; Deminter, J.; Park, J. Characterization of metals emitted from motor vehicles. Research report (Health Effects Institute) 2006, 133(133):1-76; discussion 77-88, Boston.
59. Iijima, A.; Sato, K.; Yano, K.; Tago, H.; Kato, M.; Kimura, H.; Furuta, N. Particle size and composition distribution analysis of automotive brake abrasion dusts for the evaluation of antimony sources of airborne particulate matter. *Atmos. Environ.* **2007**, *41,* 4908–4919. DOI: 10.1016/j.atmosenv.2007.02.005.

60. Liu, Y.; Xing, J.; Wang, S.; Fu, X.; Zheng, H. Source-specific speciation profiles of PM2.5 for heavy metals and their anthropogenic emissions in China. *Environ. Pollut.* **2018,** *239,* 544–553. DOI: 10.1016/j.envpol.2018.04.047.
61. Harmens, H.; and Norris, D.A. Spatial and temporal trends in heavy metal accumulation in mosses in Europe (1990–2005). Programme Coordination Centre for the ICP Vegetation, Centre for Ecology & Hydrology; Natural Environment Research Council: Bangor, UK; 2008.
62. Harmens, H.; Norris, D.A.; Koerber, G.R.; Buse, A.; Steinnes, E.; & Rühling, Å. Temporal trends in the concentration of arsenic, chromium, copper, iron, nickel, vanadium and zinc in mosses across Europe between 1990 and 2000. *Atmos. Environ.,* **2007,** *41(31),* 6673-6687. DOI:10.1016/j.atmosenv.2007.03.062.
63. Ramírez, O.; Sánchez de la Campa, A.M.; Amato, F.; Moreno, T.; Silva, L.F.; de la Rosa, J.D. Physicochemical characterization and sources of the thoracic fraction of road dust in a Latin American megacity. *Sci. Total Environ.,* **2019,** *652,* 434–446. DOI: 10.1016/j.scitotenv.2018.10.214.
64. Imperato, M.; Adamo, P.; Naimo, D.; Arienzo, M.; Stanzione, D.; Violante, P. Spatial distribution of heavy metals in urban soils of Naples city (Italy). *Environ Pollut*, **2003,** *124,* 247-256. DOI: 10.1016/s0269-7491(02)00478-5.
65. Di Vaio, P.; Magli, E.; Barbato, F.; Caliendo, G.; Cocozziello, B.; Corvino, A.; De Marco, A.; Fiorino, F.; Frecentese, F.; Onorati, G.; Saccone, I.; Santagada, V.; Soggiu, M.E.; Severino, B.; Perissutti, E. Chemical Composition of PM10 at Urban Sites in Naples (Italy). *Atmosphere,* **2016,** *7,* 163; DOI:10.3390/atmos7120163.
66. AA.,VV. Rapporto Ambientale del Piano Regionale di Gestione dei Rifiuti Urbani - CUP 894. Assessorato all'ecologia tutela dell'ambiente, programmazione e gestione dei rifiuti, tutela delle ACQUE Area Generale di Coordinamento 21 Programmazione e Gestione Rifiuti; 2011.
67. Takaoka, M.; Yamamoto, Y.; Tanaka, T.; Takeda, N.; Oshita, K.; Uruga, T. Directspeciation of lead, zinc and antimony in fly ash from waste treatmentfacilities by XAFS spectrometry, *Phys. Scr*. **2005,** *115,* 943–945. DOI: 10.1238/Physica.Topical.115a00943.
68. Sánchez-Rodasa D.; Alsioufia L.; Sánchez de la Campa, A.M.; González-Castanedo, Y. Antimony speciation as geochemical tracer for anthropogenic emissions of atmospheric particulate matter. *J. Hazard. Mater.,* **2017,** *324,* 213–220.
69. Barca, D., Comite, V., Belfiore, C.M., Bonazza, A., La Russa, M.F., Ruffolo, S.A., Crisci, G.M., Pezzino, A., Sabbioni C., Impact of air pollution in deterioration of carbonate building materials in Italian urban environments, *Appl. Geochem.,* **2014,** *48,* 122–131. DOI: 10.1016/j.apgeochem.2014.07.002.
70. Agarwal, A.; Mangal, A.; Satsangi, A.; Lakhani, A.; Maharaj Kumari, K. Characterization, sources and health risk analysis of PM2.5 bound metals during foggy and non-foggy days in sub-urban atmosphere of Agra. *Atmos. Res.,* **2017,** *197,* 121-131.
71. Liu, Y.; Xing, J.; Wang, S.; Fu, X.; Zheng, H., Source-specific speciation profiles of PM2.5 for heavy metals and their anthropogenic emissions in China. *Environ. Pollut.,* **2018,** *239,* 544-553.